REVIEWS

Journal of Semiconductors
(2020) 41, 111406
doi: 10.1088/1674-4926/41/11/111406

A survey of active quasi-circulators

Bingjun Tang and Li Geng†

School of Microelectronics, Xi'an Jiaotong University, Xi'an 710049, China

Abstract: With the development of multi-band wireless communication and the increasing data transmission rate, the circulator as an antenna interface must be able to work in multiple frequency bands and provides large bandwidth. It presents a high challenge to the design of circulators, especially the active quasi-circulators. In this survey, we review the representative active quasi-circulators and summarize three different techniques and the corresponding structures to show an incremental improvement of the isolation and bandwidth of the active quasi-circulators. In addition, we also compare the performance of several state-of-art active circulators, and analyze their advantages and disadvantages. Finally, we conclude the future trend of the active quasi-circulators.

Key words: active quasi-circulator; multiband; bandwidth; isolation; linearity; insertion loss

Citation: B J Tang and L Geng, A survey of active quasi-circulators[J]. *J. Semicond.*, 2020, 41(11), 111406. http://doi.org/10.1088/1674-4926/41/11/111406

1. Introduction

At present, the global mobile networks used in portable mobile devices such as smart phones are rapidly developing and expanding, and multi-functional smart phones are becoming more and more extensive. To meet users' real-time communication needs, the communication systems should be more effective to process text, sound and video data, and enable global roaming. In order to provide large data transmission at high data rates, multi-band wireless communication has wide range of applications in modern communication systems. Circulator is commonly used as the three-port nonreciprocal component in the radio-frequency and microwave systems in order to decouple the incident and reflected waves. As an antenna interface module, circulator should have the ability to work in multiple frequencies, that is, have the ability to work in broadband. Ferrites are the traditional materials used in the conventional passive circulators[1–3]. One of the ferrite microwave circulators was the Faraday rotation circulator, which is based on Faraday rotation, the phenomenon that occurs when microwaves of a specific polarization are incident upon a ferrite material subjected to a magnetic field parallel to the direction of propagation[4]. Because ferrite is expensive, bulky, and difficult to be integrated, in order to reduce the cost and the area of the system, active circulators are developed to replace the traditional bulky ferrite circulators.

An ideal circulator with three ports is specified as $|S_{21}| = |S_{32}| = |S_{13}| = 1$ and the other scattering parameters should be 0, as shown in Fig. 1(a). A quasi-circulator is a special type of circulator that two of its three ports (transmitter, receiver and antenna) are completely isolated in both clockwise and count-clockwise senses, as shown in Fig. 1(b), or $|S_{13}| = 0$, which means that its receiver port is isolated from its transmitter port when it is used as a duplexer. As an alternative to their ferrite counterparts, active quasi-circulators possess the advantages of small size, light weight, low cost and compatibility with the monolithic wicrowave integrated circuit (MMIC) technology.

In contrast to the multiple conventional devices, the tremendous growth of multi-band wireless communications stimulates the development of the compact and inexpensive single devices operating on multiple frequency bands, and each conventional device is assigned to a single frequency band. Circulators enable the system simultaneously transmitting and receiving the signals at different frequencies, which requires good port-to-port isolation, showing promise as an important component in wireless communication systems[4]. A software-defined radio (SDR) is a typical example of wireless communication systems where single device can operate at multiple frequency bands. The circulator replaces the functionalities of the duplexers and the switches in the SDR. The circulator is required to provide high isolation over a wide bandwidth among the receiving path (Rx), the transmitting path

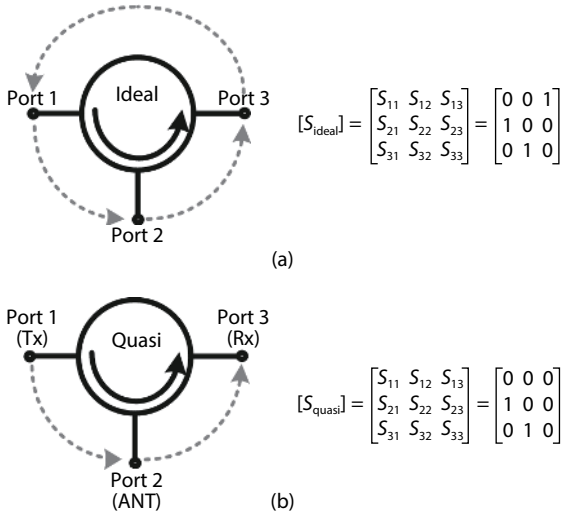

$$[S_{ideal}] = \begin{bmatrix} S_{11} & S_{12} & S_{13} \\ S_{21} & S_{22} & S_{23} \\ S_{31} & S_{32} & S_{33} \end{bmatrix} = \begin{bmatrix} 0 & 0 & 1 \\ 1 & 0 & 0 \\ 0 & 1 & 0 \end{bmatrix}$$

$$[S_{quasi}] = \begin{bmatrix} S_{11} & S_{12} & S_{13} \\ S_{21} & S_{22} & S_{23} \\ S_{31} & S_{32} & S_{33} \end{bmatrix} = \begin{bmatrix} 0 & 0 & 0 \\ 1 & 0 & 0 \\ 0 & 1 & 0 \end{bmatrix}$$

Fig. 1. Diagrams showing the *S*-parameter matrix of (a) an ideal circulator and (b) a quasi-circulator.

Correspondence to: L Geng, gengli@xjtu.edu.cn
Received 19 JULY 2020; Revised 11 SEPTEMBER 2020.

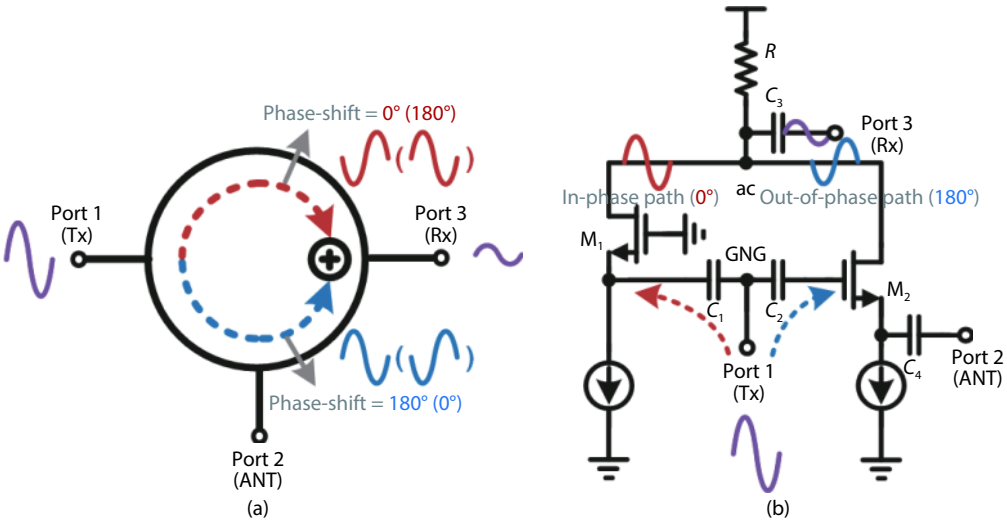

Fig. 2. (Color online) (a) Active quasi-circulator based on phase cancellation. (b) Core of conventional active quasi-circulator.

(Tx) and the antenna (ANT).

The active circulator is a key component in the future wireless systems and is responsible for multiplexing in the Tx/Rx circuits. When designing an active quasi-circulator, the key electrical parameters including frequency range, bandwidth, isolation, insertion loss, power handling, linearity and noise figure (NF) should be considered. At present, some methods and technical structures have been proposed and implemented to improve the performances of the active quasi-circulator.

2. Active quasi-circulators to improve isolation and broaden bandwidth

A common active quasi-circulator is based on phase cancellation structure[5–19], as shown in Fig. 2(a). The isolation from the Tx to the Rx is achieved by generating a cancellation signal with a phase of 180° different from the interference signal. Fig. 2(b) shows the core of conventional active quasi-circulator[20], which consists of a common-gate transistor M_1, and a common-source transistor M_2. Signals transmitted from port1 (Tx) go through two paths and are received by port3 (Rx). One is the in-phase path through M_1, and the other is the out-of-phase path through M_2. When the signals from two paths meet at the resistor R, two paths of signals could be cancelled by each other. However, since the phase difference and the amplitude of the signals vary with the frequency after the signals pass through the in-phase path and the out-of-phase path, the common active quasi-circulator achieves high isolation within a limited bandwidth[21].

In order to improve the isolation performance over a wide bandwidth, especially the isolation of the Tx port (port 1) to the Rx port (port 3), i.e., S_{31}, the tunable architectures and wideband architectures were proposed. These two main types of active quasi-circulators have their own advantages and disadvantages. The tunable active quasi-circulator can achieve high isolation performance but with limited bandwidth. In contrast, the wideband active quasi-circulator operates over a wide bandwidth, while the isolation S_{31} is usually not high enough.

2.1. Tunable architectures

The adjustable discrete components have achieved excellent narrow-band performance over a wide frequency range, which is common in quasi-circulators for multi-band wireless communication systems. By adding a tunable capacitor to a signal path of the circulator, as shown in Fig. 3(a), the capacitance value can be tuned according to the different frequencies to realize the adjustment of the phase of this path. By this way, the phase difference between the in-phase path and the out-of-phase path at different frequencies can be maintained near 180°, thereby ensuring the high isolation (S_{31}). As shown in Fig. 3(b), high isolation can be obtained at multi-frequencies by tuning the capacitance. Fig. 3(c) shows the schematic of a tunable active quasi-circulator[22]. For a quasi-circulator, power is transferred unidirectionally between two pairs of ports, and the third pair is isolated. Port 1 is the Tx signal, port 2 is the antenna (ANT), and port 3 is the Rx signal in a radio system. The tunable active quasi-circulator achieves Tx gain (S_{21}) using a distributed amplifier (DA) composed of M_2, M_4 and M_5. While the output currents from the gain stages are directly added to the ANT port, the reverse wave from the second stage and the co-directional wave from the first stage are cancelled at the Rx port. High isolation is maintained across a relatively wide frequency range through tuning of a shunt capacitor bank between this two amplifier stages to ensure the out-of-phase cancelation. The gains can also be individually tuned to offset the frequency-dependent line losses.

The measured results show that the isolation (S_{31}) exhibits nulls from 5.3 to 7.3 GHz ranging from 42 dB near the center frequency to 30 dB at the band edge, with a 20 dB cancelation bandwidth of 400 MHz. Tx gain (S_{21}), RX insertion loss (S_{32}), return losses (S_{11}, S_{22}, S_{33}), and reverse isolation (S_{12}) vary by less than 0.5 dB with respect to shunt capacitance.

Another tunable active quasi-circulator is shown in Fig. 4(a). The phase adjustment of the signal transmission path is realized by replacing the tunable capacitor with the T-network phase shifters. The detailed circuit structure of this tunable active quasi-circulator is shown in Fig. 4(b)[4, 23]. It is formed by connecting three single-stage distributed amplifiers (DAs) together with a T-network phase shifter. Two of the single-stage DAs (DA1 and DA2) are for wideband transmission, and the third one (DA3) is for wideband signal cancella-

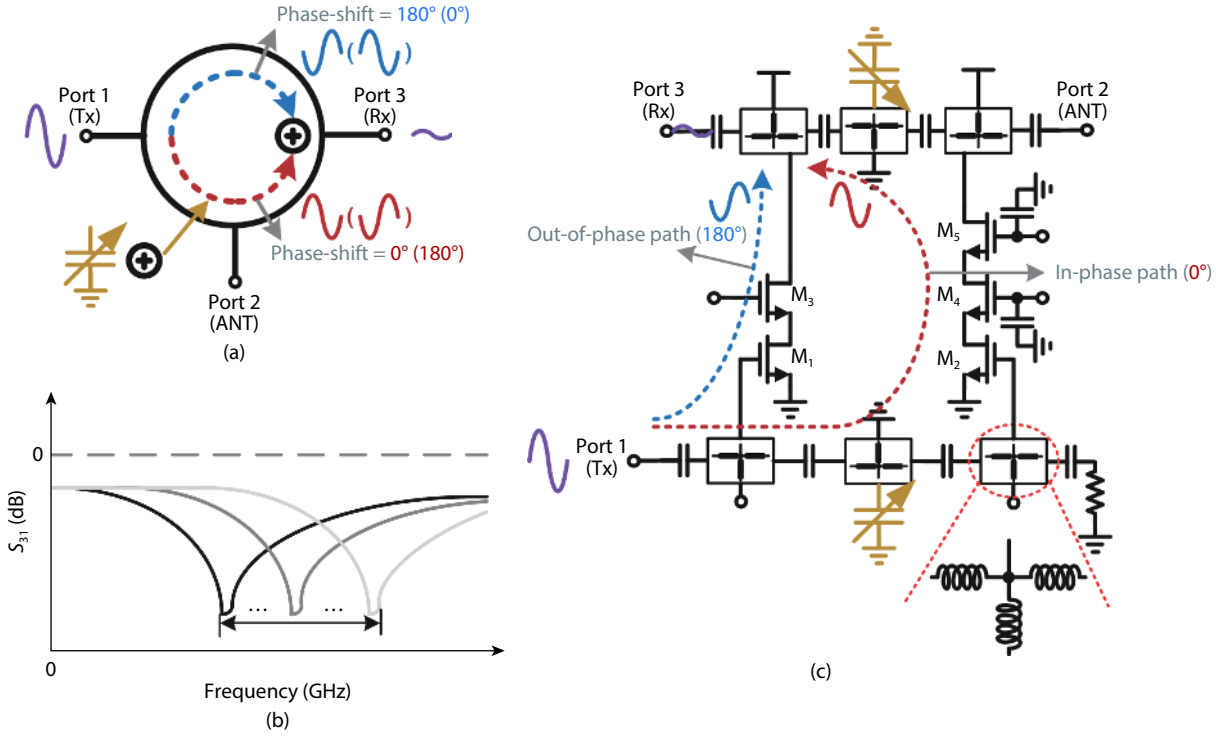

Fig. 3. (Color online) (a) Active quasi-circulator with a tunable capacitor. (b) Isolation S_{31} varies with frequency. (c) Schematic of a tunable distributed active quasi-circulator.

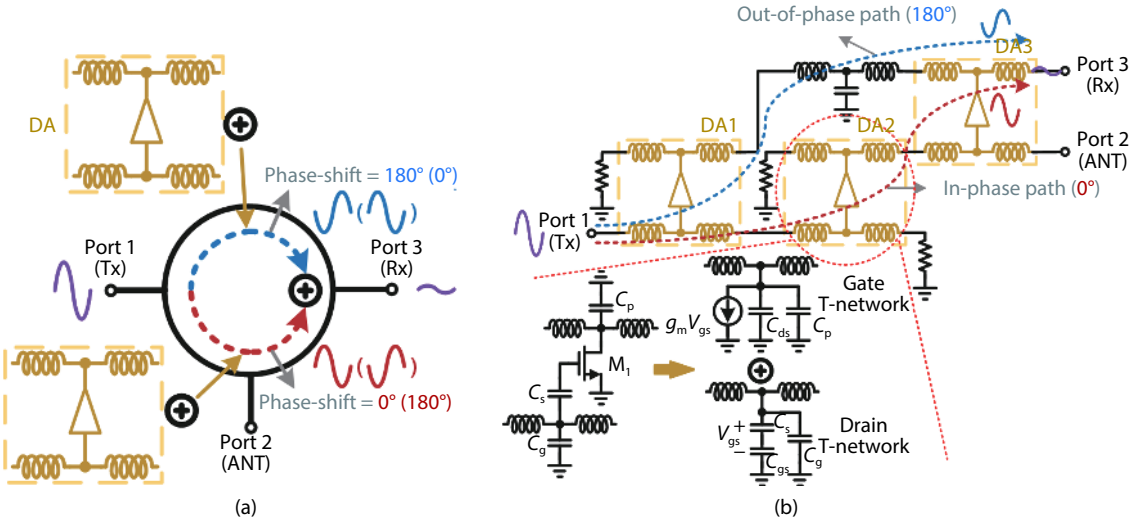

Fig. 4. (Color online) (a) Tunable active quasi-circulator with T-network phase shifters. (b) Schematic of the tunable active quasi-circulator by using DAs.

tion between path 1 and path 2 to achieve wideband isolation between port 1 and port 3[9]. The other port-isolation is mainly due to the unilateral characteristics of the transistors. Because the power and phase response of the single-stage DAs are not sufficiently flat within the bandwidth, gate-to-source capacitance C_{gs}, drain-to-source capacitance C_{ds}, and transconductance g_m for each DA are optimized to achieve good isolation between port 1 and port 3[4]. The parameters are optimized by tuning the bias current of the transistor in each DA.

The measured tunable isolation between port 1 and port 3 shows wideband isolation with the minimum isolation of around 15 dB from 0.8 to 2.2 GHz, and the tunable isolation is more than 40 dB at ω_o over the frequency range of 0.8–2.2 GHz. And the insertion losses and return losses are about 0 ± 1.5 dB and better than 10 dB, respectively.

Although the above two tunable active quasi-circulators obtain good isolation within a certain frequency range, the phase shifters based on tunable capacitor or T-network are narrowband devices. The corresponding bandwidth is still narrowed within near the specific adjustment point. The relatively narrow bandwidth does not satisfy the high data rate and large bandwidth requirements of 5G and future 6G wireless communications.

2.2. Wideband active quasi-circulators

To improve the isolation and bandwidth of the active quasi-circulator, the feedback technology[21], the dual techno-

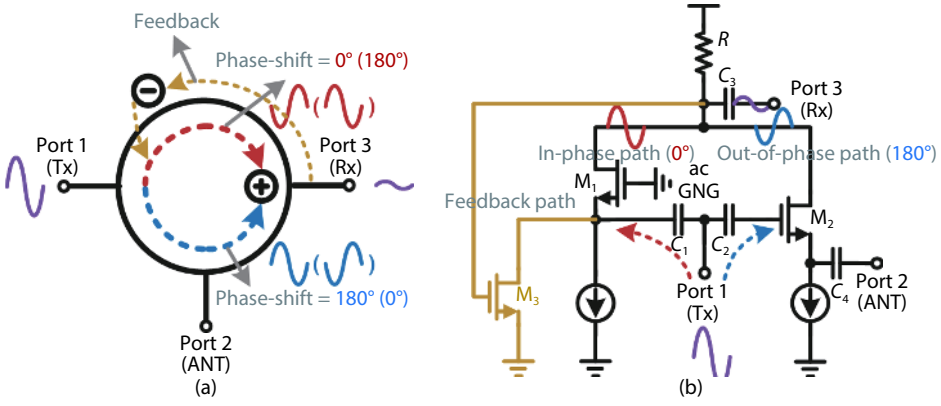

Fig. 5. (Color online) (a) Active quasi-circulator with feedback technology. (b) Core circuit of feedback active quasi-circulator.

logy[24] and the advanced dual technology[25] are proposed and designed, successively.

2.2.1. Feedback technology

Feedback technology is commonly used in various circuit designs to increase the bandwidth and improve the circuit stability. In Ref. [21], the isolation from the transmitter to the receiver (S_{31}) can be enhanced by adding a feedback path from port 3 to the cancellation signal path based on the common active circulator shown in Fig. 5(a). The circuit structure of the feedback active quasi-circulator is shown in Fig. 5(b), which is based on the conventional circuit structure shown in Fig. 2. M_3 is added in the circuit to constitute a feed-back path.

According to Figs. 2 and 5, $|S_{31c}|$ of the conventional active quasi-circulator and $|S_{31f}|$ of the feedback active quasi-circulator are obtained, respectively, and can be expressed as[21]:

$$|S_{31c}| = |S_{31f}| \cdot \alpha, \tag{1}$$

where $\alpha \approx \left|\frac{R_S}{2} + \frac{g_{m3}R_S^{\,2}}{24} + \frac{5g_{m3}R_S^{\,2}}{24 + 48R_SC_1S}\right| > \left|\frac{R_S}{2}\right| > 1$, and R_S is the characteristic impedance, i.e., 50 Ω in this work.

The denominator part of $|S_{31f}|$ contains the square term of S in Ref. [21]. So when the frequency increases, the denominator increases fast, causing the value of $|S_{31f}|$ decrease more rapidly comparing with that of $|S_{31c}|$, especially at the high frequency range[21]. No matter how the frequency changes, $|S_{31f}|$ is α times smaller than $|S_{31c}|$. This means that the circulator with feedback can achieve higher isolation and wider bandwidth than that without feedback.

The measured $|S_{31}|$ is higher than 27 dB over a frequency range from 0.8 to 6.8 GHz. The measured $|S_{12}|$ is higher than 15 dB, while $|S_{23}|$ and $|S_{13}|$ are all larger than 20 dB. The measured $|S_{21}|$ (insertion loss from Tx to antenna (ANT in Fig. 4)) is between −8 and −10 dB, while the measured $|S_{32}|$ (from antenna to Rx) is between −9 and −12 dB.

2.2.2. Dual technology

In order to further improve the isolation and bandwidth, the dual structure has been proposed, as shown in Fig. 6(a). Another cancellation signal (dual signal) is added in the dual structure, and the schematic of the dual interference-cancelling active quasi-circulator is shown in Fig. 6(c)[24]. The conventional active quasi-circulator with buffer is shown in Fig. 6(b)[20]. The input signal from port 1 passes through the primary cancellation circuit, which is composed of M_1 and M_2, as shown in Fig. 6(b), and the dual circuits are composed of M_{1d} and M_{2d}. Signals obtained after passing the primary and dual circuits are identical, and they meet at port 3 through the in-phase source-follower M_3 and the anti-phase common-source M_4, respectively, with achieved higher isolation. Port 2d is terminated by a 50 Ω off-chip resistor to ensure symmetry and acts as a dummy port[24].

The isolation from transmitter to receiver, represented by S_{31}, is the most important performance of the active quasi-circulators. According to Figs. 6(b) and 6(c), $|S_{31cc}|$ of the conventional active quasi-circulator and $|S_{31d}|$ of the dual active quasi-circulator are obtained, respectively, and can be expressed as:

$$S_{31cc} = 2\frac{Z_1}{R_S + Z_1}\frac{g_{m3}Z_3}{1 + g_{m3}Z_3}\left(\frac{g_{m1}R}{1 + \dfrac{g_{m1}}{C_1S}} - \frac{g_{m2}R}{1 + g_{m2}Z_a}\right) = 2AB(C - D), \tag{2}$$

$$S_{31d} \approx S_{31cc} - 2\frac{Z_1||Z_{1d}}{R_s + Z_1||Z_{1d}}\left[\frac{g_{m4}Z_3}{1 + g_{m4}Z_3}\left(\frac{g_{m1d}R_d}{1 + \dfrac{g_{m1d}}{C_{1m}S}} - \frac{g_{m2d}R_d}{1 + g_{m2d}Z_{ad}}\right)\right] \tag{3}$$

$$= S_{31cc} - 2AB(E - F),$$

where $Z_1 = 1/g_{m1} + 1/C_1S$, $Z_{1d} = 1/g_{m1d} + 1/C_{1d}S$, $Z_3 = R_S + 1/C_LS$, $Z_{ad} = R_S + 1/C_{ad}S$, and $R_S = 50$ Ω. $|S_{31d}|$ is roughly improved by $2AB(E–F)$.

In addition, the two terms in Eq. (2), C and D, vary with frequency, resulting in cancellation within a relatively small frequency range, and hence a narrow isolation bandwidth. On the contrary, the two terms in Eq. (3), $C - D$ and $E - F$, achieve a much better cancellation versus frequency, given that the circuits represented by the two terms are almost identical[24]. Bandwidth and isolation can be simultaneously enhanced.

The measured isolation $|S_{31}|$ is better than 36 dB within bandwidth of 6 GHz. The measured insertion loss $|S_{21}|$ (from transmitter to antenna) and $|S_{32}|$ (from antenna to receiver) are below 10 and 9 dB from 1 to 7 GHz, respectively. Matching at Tx could be improved by adding additional impedance matching circuits.

2.2.3. Advanced dual technology

Due to the problem of large insertion loss and large

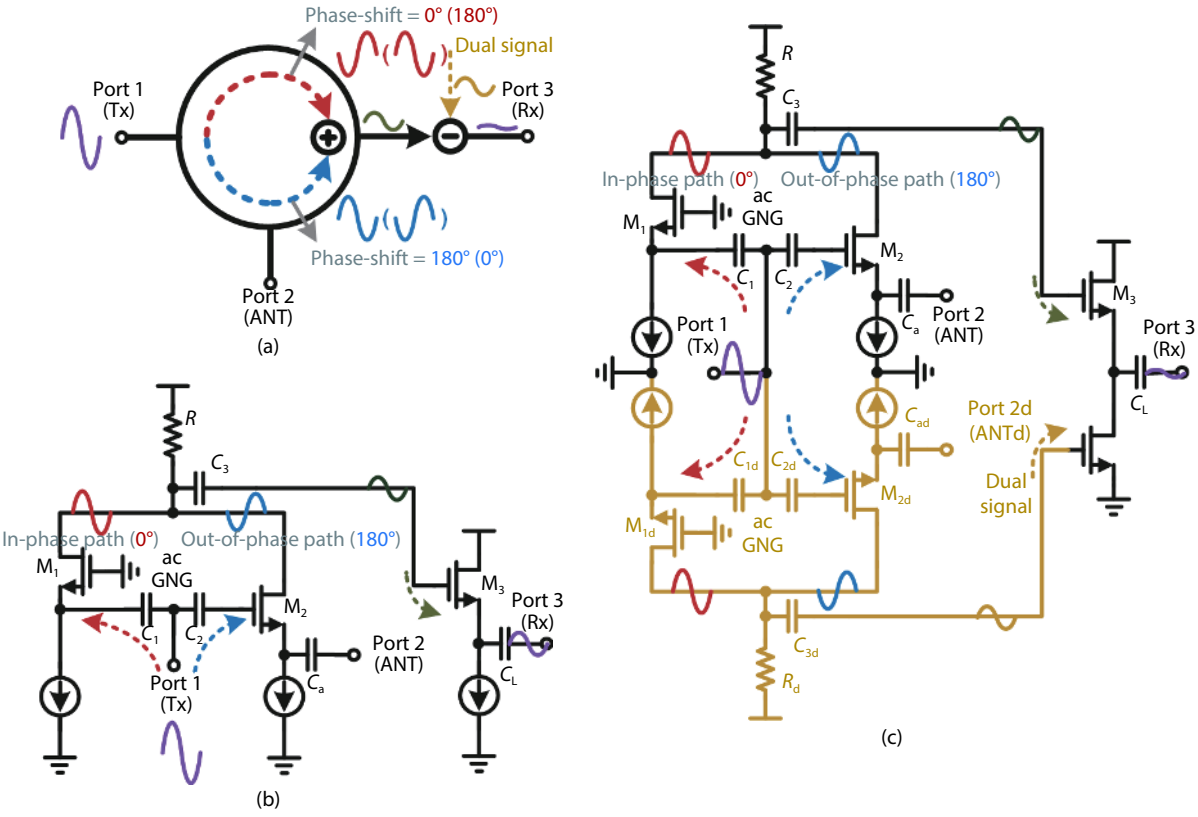

Fig. 6. (Color online) (a) Active quasi-circulator with dual technology. (a) Architecture of conventional active quasi-circulator. (b) Schematic of dual interference-cancelling active circulator.

noise figure of the dual active quasi-circulator[24], an advanced dual structure active quasi-circulator based on the insertion loss and noise reduction technology is proposed[25]. The advanced dual structure is basically relied on the dual cancellation signals, as shown in Fig. 7(a), and the schematic of the advanced dual quasi-circulator is shown in Fig. 7(b)[25]. It consists of two common-source transistors (M_2 and M_{2E}), one common-gate transistor (M_1), a g_m-boosted transistor (M_g) and a symmetric isolation buffer circuitry (source-follower transistors M_{B1}/M_{B2}, and common-source transistors M_{B3}/M_{B4}). The g_m-boosted circuit (M_g and R_g) improves the effective transconductance of M_1, which is equal to $g_{m1}(1+g_{mg}R_g)$[25]. The impedance of port 1 is determined by $1/[g_{m1}(1+g_{mg}R_g)]$. The impedances of port 2 and port 3 are determined by the transconductance of M_2 and M_{B1}/M_{B2}, respectively. All three ports are designed to show 50 Ω impedance. Port 2d is terminated by a 50 Ω off-chip resistor to ensure the symmetry, acting as a dummy port.

The interference signal generated by the Tx signal through the out-of-phase path (M_2) and the buffer (M_{B1}) is suppressed by the cancellation signal generated from the Tx through the in-phase path (M_1) and the buffer (M_{B2}), which produces a residual signal. The dual cancellation signal is introduced in the advanced dual-path topology to further cancel the residual signal. The dual cancellation signal is generated by the Tx signal through the in-phase path (M_1), the buffer (M_{B4}), the out-of-phase path (M_{2E}) and the buffer (M_{B3}). The insertion loss is critical since the NF is partially dependent on it. The load resistor is degraded by both the finite output impedances of M_1 and M_2, and hence decreases the gain and deteriorates the NF[24]. Relying on the proposed insertion loss mitigation technique shown in Fig. 7(b), the load resistor R is degraded by only one finite output impedance of M_2 by employing the symmetric isolation buffers to avoid the gain reduction impact from the finite output impedance of M_1 in the in-phase path. In addition, since the current flowing through the load resistor in Ref. [24] is twice of that flowing through R_2 in this design, to ensure the linearity of these two topologies similar, R_2 can be designed to be twice the load resistor of Ref. [24].

The insertion losses of Ref. [24] and the advanced topology are given as S'_{32} and S_{32}, respectively. Comparing S'_{32} with S_{32}, Eq. (4) can be obtained

$$S_{32} \approx \frac{Z_2 Z_L^2}{Z'_2 Z'^2_L} \cdot S'_{32}, \tag{4}$$

where $Z'_2 = 1/g'_{m2} + 1/C'_aS$, $Z'_L \approx ro'_1||ro'_2||R'$, $R' = 100$ Ω, $ro'_1 \approx ro'_2 \approx 500$ Ω, $Z_2 = R_S + 1/C_aS$, $Z_L = ro_2||R_2$, $R_2 = 200$ Ω, $ro_2 \approx 500$ Ω, $R_S = 50$ Ω. Through the above analysis, $S'_{32} < S_{32}$ can be obtained.

The isolation from Tx to Rx (S_{31}) can be defined as the difference between the transmission losses from port 1 to port 2 (TX-ANT) and from port 1 to port 3 (TX-RX). The measured $|S_{21}|$ and $S_{32}|$ are below 8 and 2.5 dB from 1 to 8 GHz, respectively. The measured $|S_{31}|$ is better than 34 dB from 1 to 8 GHz. Compared with the dual technology, the advanced dual technology has improved $|S_{21}|$ and $|S_{32}|$ by 2 and 6.5 dB, respectively.

Although the above three technologies have effectively

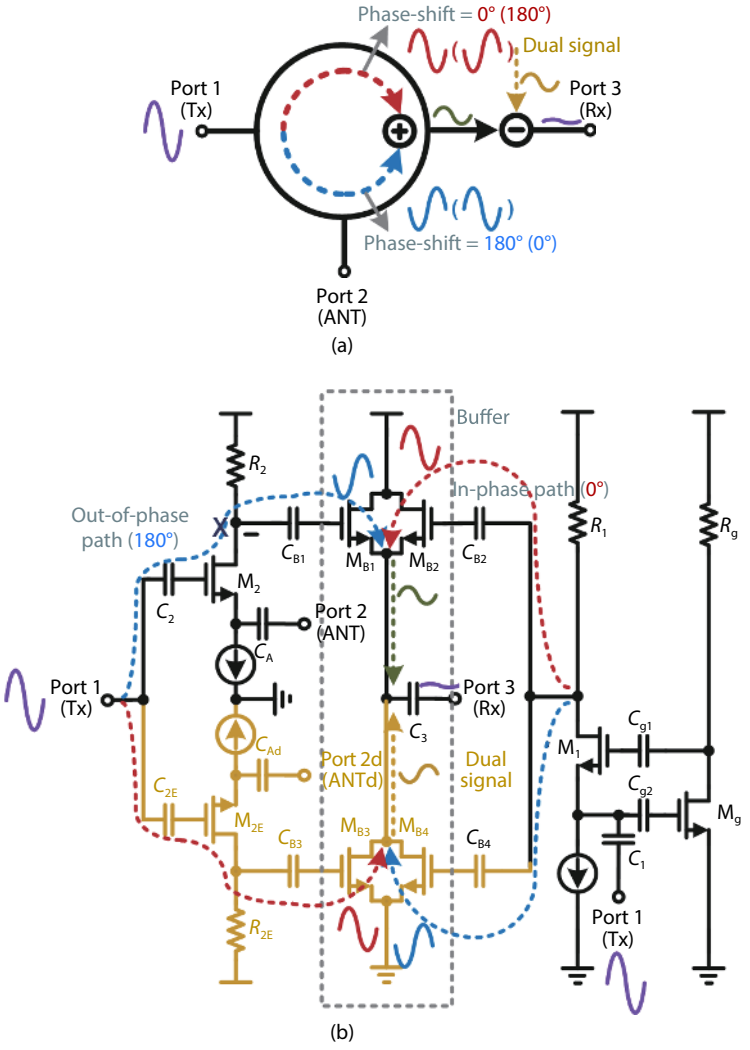

Fig. 7. (Color online) Architecture of advanced dual interference-cancelling active circulator.

improved the isolation and the bandwidth of the active quasi-circulators, there are still problems of insufficient linearity, large insertion loss, and large noise figure. These problems will limit its application in 5G and future 6G communications.

3. Structures to improve power handling, linearity and noise figure (NF)

The most common approach adopted in the quasi-circulator designs to improve power handling, linearity and noise figure is based on the linear periodically-time-varying (LPTV) architecture[26–32]. Linear time varying (LTV) systems can be non-reciprocal. Two-port N-path filters with a phase-shift between the input and output clocks have been explored as means of adding phase shift to signals traveling through the filter[32]. This phase non-reciprocity behavior can also be intuitively understood by viewing the two sets of switches as reciprocal quadrature mixers, and viewing the baseband capacitors together with the source resistance at the two ports as a low-pass filter[26]. In the LTV active quasi-circulator, one signal path is replaced by a 3λ/4 transmission line achieving 270° phase shift, and cancellation signal path is replaced by the reciprocal quadrature mixers with 90° phase shift, so that the phase difference of the two paths is 180°, which is very adapted to achieve interference signal cancellation, as shown in Fig. 8(a). LPTV analysis shows that this introduces constant phase shifts near the switching clock frequency (f_{LO}) with no other impacts on the close-in magnitude response[33]. The low-pass filter attenuates the up-converted signal from the first mixer in either propagation direction. The phase non-reciprocity is achieved by the different roles that the phase-shifted clocks play in different signal propagation directions: the phase-shifted clocks act as up-conversion local oscillators in the left to right direction, and act as down-conversion local oscillators in the right to left direction.

A 3λ/4 transmission line is wrapped around the N-path filter with 90° clock phase shift to create non-reciprocal wave propagation. In this ring, signals can only propagate in one direction. In the clockwise direction in Fig. 8(b)[26], the –270° phase shift of the 3λ/4 line combines with the –90° shift of the N-path filter to create co-directional interference. For the counter-clockwise, the –270° phase shift of the 3λ/4 line adds with the 90° shift of the N-path to create reverse interference. The 3λ/4 transmission line is miniaturized using three CLC sections that is equivalent to a λ/4 transmission line.

The measured in-band Tx-ANT and ANT-Rx IIP3 are 27.5 dBm and 8.7 dBm, respectively. The ANT-Rx NF is 4.3 dB, while the Tx-to-Rx isolation is better than 42 dB across 12 MHz bandwidth. The measured results show that the LPTV

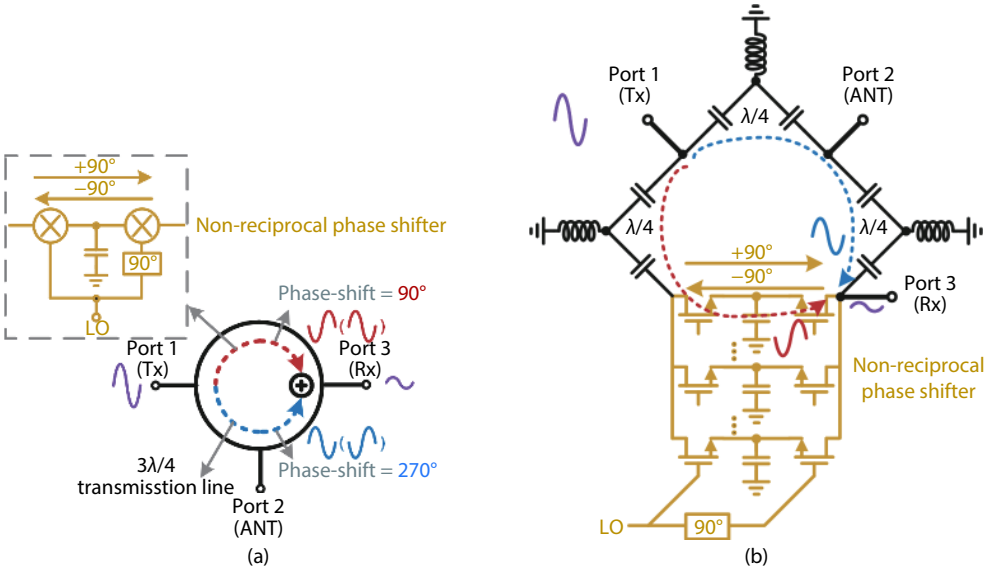

Fig. 8. (Color online) (a) LPTV active quasi-circulator. (b) Three-port circulator with a 3λ/4 transmission-line ring.

Table 1. Comparison with published active quasi-circulators.

Parameter	MWCL 2010[8]	ISSCC 2015[34]	JSSC 2015[35]	ISSCC 2016[26]	ISSCC 2017[28]	MWCL 2017[22]	IWS 2018[21]	MWCL 2019[24]	MWCL 2020[25]
Technology	180 nm CMOS	180 nm CMOS	65 nm CMOS	65 nm CMOS	45 nm CMOS SOI	45 nm CMOS SOI	180 nm CMOS	180 nm CMOS	180 nm CMOS
Frequency (GHz)	29–31	1.9–2.2	0.1–1.5	0.6–0.8	22.7–27.7	5.3–7.3	0.8–6.8	1–7	1–8
Bandwidth (%)	7	15	175	29	20	32	158	150	156
$\|S_{31}\|$ (dB)	12	50	30	15	18.5	30	27	36	34
$\|S_{21}\|$ (dB)	4–6	3.7	NA	2.5	3.3	10.5 (gain)	8–10	10	8
$\|S_{32}\|$ (dB)	7.2–7.9	3.9	0	2.5	3.2	5	9–12	9	2.5
$\|S_{23}\|$ (dB)	24	NA	NA	NA	5	NA	28	30	16
$\|S_{12}\|$ (dB)	22	NA	NA	2.5	7	25	20	15	34
$\|S_{13}\|$ (dB)	35	NA	NA	NA	8	NA	15	30	33
$\|S_{11}\|$ (dB)	6	NA	20	5	10	10	3	6	8.5
$\|S_{22}\|$ (dB)	5	NA	NA	5	10	10	5	10	11
$\|S_{33}\|$ (dB)	11.5	NA	NA	NA	14	10	5	11	8.5
Tx-ANT IIP3 (dBm)	NA	70	NA	27.5	19.9	20	7.37	9.7	9
ANT-Rx IIP3 (dBm)	NA	NA	NA	8.7	20	NA	2.43	3.5	4.2
ANT-RX NF (dB)	NA	NA	5.5	4.3	3.3–4.4	20	20	16–20	9–10
Area (mm^2)	0.41	1.75	1.5	1.4	2.6	1.57	0.3564	0.5665	0.45
P_{DC} (mW)	15	NA	43–56	30	378.4	4.5	12.8	25.2	24.8

structure helps the active quasi-circulator to obtain relatively high linearity and relatively low NF.

Even though the active quasi-circulator based on the LPTV structure has good linearity, noise figure and high power processing capability, it cannot be used for broadband because of the narrowband characteristics of the LPTV structure. Therefore, it is not very suitable for the future high-speed and broadband wireless communications.

4. Comparison and future design trends of active quasi-circulators

Table 1 shows the comparison of the recently published active quasi-circulators, including the above mentioned six active quasi-circulators. For the wideband quasi-circulators[21, 24, 25, 35] with a bandwidth over 100%, the isolation performance is about 30 dB, with relatively high insertion loss and noise coefficient, and insufficient linearity. For the narrow band quasi-circulators[8, 22, 26] with a bandwidth below 50%, the insertion loss is about 5 dB and it has a relatively low isolation.

With the development trend of the portable wireless communication systems, circulators should be miniaturized and highly integrated. Since ferrite passive circulators are large and difficult to be highly integrated, active quasi-circulators could be the mainstream of future development. And with the huge development of multi-band wireless communication, the circulator as an antenna interface must have the ability to work in broadband. Fig. 9 shows the bandwidth and isolation behaviors of the active quasi-circulator designs. Most active quasi-circulators are based on phase cancellation strategy. Since the phase difference and the amplitude of the signals vary with the frequency after the signals pass through the in-phase path and the out-of-phase path, most active quasi-circulators achieve high isolation within a limited bandwidth[21]. And most of the current active quasi-circulator designs are still in the region of narrow band and have low isolation. Al-

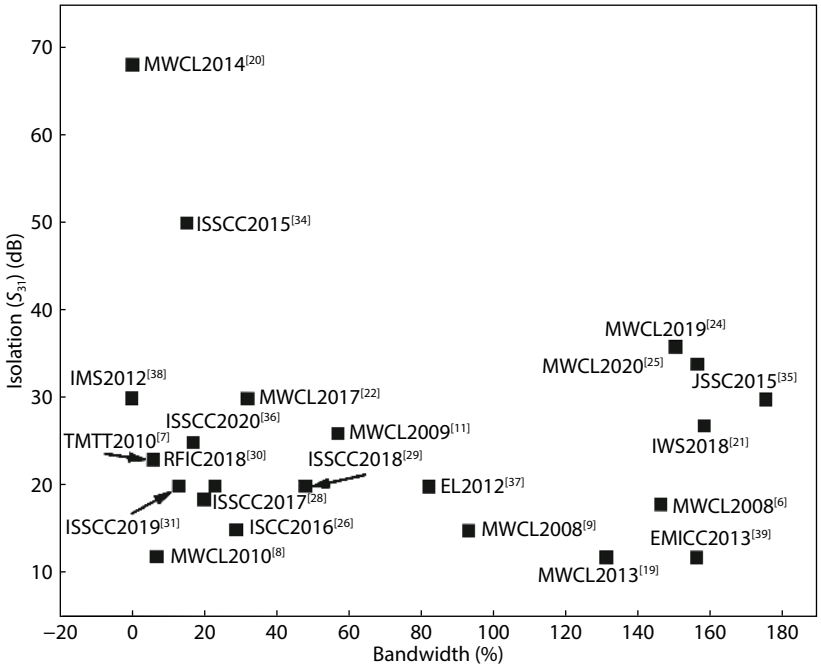

Fig. 9. Bandwidth and isolation behaviors of state of art active quasi-circulators.

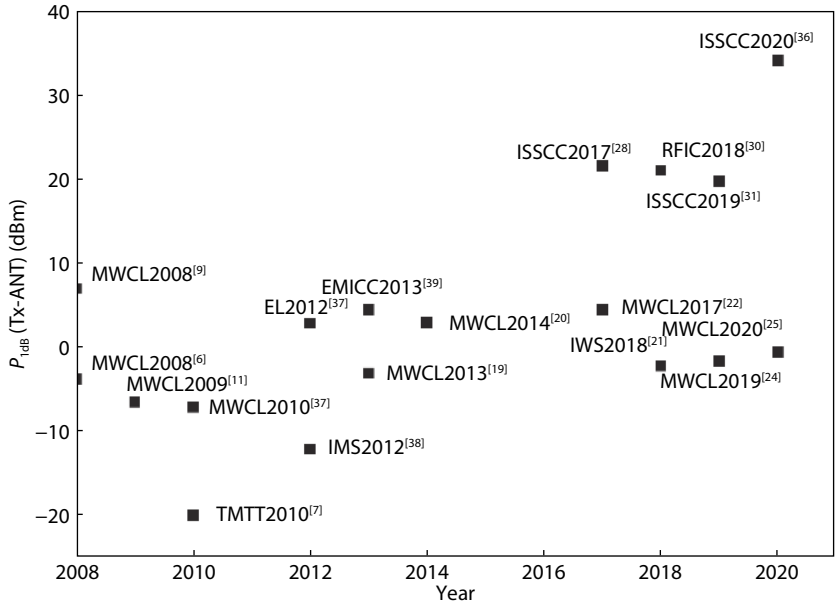

Fig. 10. Linearity behaviors of state of art active quasi-circulators.

though the tunable technology can enhance the isolation in multiple frequency bands, its relatively narrow bandwidth limits its applications in the future high-data and large-bandwidth communications. At present, the feedback technology, dual technology and advanced dual technology have been introduced into the design of active circulators to break the difficulty of possessing high isolation and broadband at the same time. However, even though the feedback technology, dual technology and advanced dual technology make better balance between the large bandwidth and high isolation of the active quasi-circulator, there are still the problems of insufficient linearity and excessive noise. Fig. 10 displays the trend in linearity for active quasi-circulators. High linearity is required, more new designs are focus on it. Meanwhile, although the active quasi-circulator based on LPTV architecture[36] can obtain relatively high linearity, low noise and low insertion loss, but the isolation and the bandwidth are insufficient.

Therefore, to satisfy the performance of high isolation, broadband and high linearity at the same time presents a huge design challenge for active quasi-circulators in the future. Solving this problem will accelerate the full replacement of passive circulators by the active circulators, which will bring a great advancement in the high integrated wireless communication systems. Through analyzing the prior methods of how to improve the isolation, bandwidth, power processing, linearity and noise figure, discussing the compromise among the various performances and the performance distribution of the existing state of arts shown in Figs. 9 and 10, respectively, the following five aspects are feasible directions

for the future research of active quasi-circulators, and all these aspects show great challenges.

(1) Expanding bandwidth. With the development of 5G communication and 6G communication in the future, the demands for broadband active quasi-circulators will increase rapidly. Most active quasi-circulators are based on phase cancellation. If the in-phase path and the out-of-phase path have the same frequency response, a large bandwidth can be obtained.

(2) Improving isolation. The circulator should have high degree of Tx-Rx isolation, which could greatly reduce the interference of the signal at transmitter to the signal at receiver, and will reduce the linearity requirement of the receiver. If the in-phase path and the out-of-phase path have the same amplitude response and the phase difference is exactly 180°, a very high degree of isolation can be guaranteed.

(3) Reducing insertion loss. Reducing the insertion loss of the active quasi-circulator will improve the transmission efficiency of the transmitter and save the power consumption, and will reduce the noise of the receiver. Reducing insertion loss can be achieved by adding buffers and power amplifiers in the output path, or by optimizing the circuit structure to reduce the loss on the signal transmission path.

(4) Improving linearity. Linearity is currently the key restriction of the passive circulators being replaced by the active quasi-circulators. The input reference P_{1dB} of the active circulator needs to reach more than 30 dBm, which presents a very big challenge. The linearity can be improved by using high power-supply transistors or GaN devices, and the new structures like LPTV can also be used to improve the linearity.

(5) Reducing noise figure. The active quasi-circulator is the front end of the receiving link, and its noise contributes mostly to the noise figure of the entire link. Reducing the noise figure is another challenge in designing the active quasi-circulator. To reduce the noise figure, the design method similar to that of a low-noise amplifier can be adopted. On the one hand, the number of transistors on the signal transmission path should be reduced, and on the other hand, the gain on the signal transmission path need to be increased, and other noise cancellation technologies can also be applied.

5. Conclusion

As an antenna interface for multi-band wireless communications, the circulator must be capable to operate in multiple frequency bands, and at the same time it should have a large operating bandwidth. This survey reviews several existing structures of active quasi-circulators, and technical methods used to improve the bandwidth, isolation, linearity and noise performance. The advanced dual technology can effectively improve the isolation and bandwidth of the active quasi-circulator. The LPTV structure can be used to improve the linearity and noise performance. Better tradeoff among high isolation, broadband and good linearity needs to be made, which is always the direction of designing active quasi-circulators. Finally, the methods, which are useful to enhance the features of the active quasi-circulators, are provided to be the good references to the future works.

References

[1] Fathy A, Denlinger E, Kalokitis D, et al. Miniature circulators for microwave superconducting systems. Proceedings of 1995 IEEE MTT-S International Microwave Symposium, 1995, 195

[2] Yung E K N, Chen R S, Wu K, et al. Analysis and development of millimeter-wave waveguide-junction circulator with a ferrite sphere. IEEE Trans Microw Theory Tech, 1998, 46, 1721

[3] Borjak A M, Davis L E. More compact ferrite circulator junctions with predicted performance. IEEE Trans Microw Theory Tech, 1992, 40, 2352

[4] Mung S W Y, Chan W S. The challenge of active circulators: Design and optimization in future wireless communication. IEEE Microw Mag, 2019, 20, 55

[5] Hara S, Tokumitsu T, Aikawa M. Novel unilateral circuits for MMIC circulators. IEEE Trans Microw Theory Tech, 1990, 38, 1399

[6] Shin S C, Huang J Y, Lin K Y, et al. A 1.5–9.6 GHz monolithic active quasi-circulator in 0.18 μm CMOS technology. IEEE Microw Wirel Compon Lett, 2008, 18, 797

[7] Wu H S, Wang C W, Tzuang C K C. CMOS active quasi-circulator with dual transmission gains incorporating feedforward technique at K-band. IEEE Trans Microw Theory Tech, 2010, 58, 2084

[8] Chang C H, Lo Y T, Kiang J F. A 30 GHz active quasi-circulator with current-reuse technique in 0.18 μm CMOS technology. IEEE Microw Wirel Compon Lett, 2010, 20, 693

[9] Mung S W Y, Chan W S. Novel active quasi-circulator with phase compensation technique. IEEE Microw Wirel Compon Lett, 2008, 18, 800

[10] Gasmi A, Huyart B, Bergeault E, et al. Noise and power optimization of a MMIC quasi-circulator. IEEE Trans Microw Theory Tech, 1997, 45, 1572

[11] Zheng Y, Saavedra C E. Active quasi-circulator MMIC using OTAs. IEEE Microw Wirel Compon Lett, 2009, 19, 218

[12] Kalialakis C, Cryan M J, Hall P S, et al. Analysis and design of integrated active circulator antennas. IEEE Trans Microw Theory Tech, 2000, 48, 1017

[13] Palomba M, Bentini A, Palombini D, et al. A novel hybrid active quasi-circulator for L-band applications. 2012 19th International Conference on Microwaves, Radar & Wireless Communications, 2012, 41

[14] Huang D J, Kuo J L, Wang H E. A 24-GHz low power and high isolation active quasi-circulator. 2012 IEEE/MTT-S International Microwave Symposium Digest, 2012, 1

[15] Hung S H, Lee Y C, Su C C, et al. High-isolation millimeter-wave subharmonic monolithic mixer with modified quasi-circulator. IEEE Trans Microw Theory Tech, 2013, 61, 1140

[16] Wang S, Lee C H, Wu Y B. Fully integrated 10-GHz active circulator and quasi-circulator using bridged-T networks in standard CMOS. IEEE Trans VLSI Syst, 2016, 24, 3184

[17] Ghosh D, Kumar G. A broadband active quasi circulator for UHF and L band applications. IEEE Microw Wirel Compon Lett, 2016, 26, 601

[18] Mung S W Y, Chan W S. Self-equalization technique for distributed quasi-circulator. Microw Opt Technol Lett, 2009, 51, 182

[19] Hung S H, Cheng K W, Wang Y H. An ultra wideband quasi-circulator with distributed amplifiers using 90 nm CMOS technology. IEEE Microw Wirel Compon Lett, 2013, 23, 656

[20] Hsieh J Y, Wang T, Lu S S. A 1.5-mW, 2.4 GH_z quasi-circulator with high transmitter-to-receiver isolation in CMOS technology. IEEE Microw Wirel Compon Lett, 2014, 24, 872

[21] Tang B J, Xu J T, Geng L. Integrated active quasi-circulator with 27 dB isolation and 0.8–6.8GHz wideband by using feedback technique. 2018 IEEE MTT-S International Wireless Symposium (IWS), 2018, 1

[22] Fang K, Buckwalter J F. A tunable 5 –7 GHz distributed active quasi-circulator with 18-dBm output power in CMOS SOI. IEEE Microw Wirel Compon Lett, 2017, 27, 998

[23] Mung S W Y, Chan W S. Wideband active quasi-circulator with tunable isolation enhancement. J Eng, 2014, 2014, 83

[24] Tang B J, Gui X Y, Xu J T, et al. A dual interference-canceling active quasi-circulator achieving 36-dB isolation over 6-GHz bandwidth. IEEE Microw Wirel Compon Lett, 2019, 29, 409

[25] Tang B J, Gui X Y, Xu J T, et al. A wideband active quasi-circulator with 34-dB isolation and insertion loss of 2.5 dB. IEEE Microw Wirel Compon Lett, 2020, 30, 693

[26] Zhou J, Reiskarimian N, Krishnaswamy H. Receiver with integrated magnetic-free N-path-filter-based non-reciprocal circulator and baseband self-interference cancellation for full-duplex wireless. 2016 IEEE International Solid-State Circuits Conference (ISSCC), 2016, 178

[27] Reiskarimian N, Zhou J, Krishnaswamy H. A CMOS passive LPTV nonmagnetic circulator and its application in a full-duplex receiver. IEEE J Solid-State Circuits, 2017, 52, 1358

[28] Dinc T, Krishnaswamy H. 17.2 A 28 GHz magnetic-free non-reciprocal passive CMOS circulator based on spatio-temporal conductance modulation. 2017 IEEE International Solid-State Circuits Conference (ISSCC), 2017, 294

[29] Jain S, Agrawal A, Johnson M, et al. A 0.55-to-0.9 GHz 2.7 dB NF full-duplex hybrid-coupler circulator with 56 MHz 40 dB TX SI suppression. 2018 IEEE International Solid-State Circuits Conference - (ISSCC), 2018, 400

[30] Nagulu A, Alù A, Krishnaswamy H. Fully-integrated non-magnetic 180nm SOI circulator with > 1W P_{1dB} >+50dBm IIP_3 and high isolation across 1.85 VSWR. 2018 IEEE Radio Frequency Integrated Circuits Symposium (RFIC), 2018, 104

[31] Nagulu A, Krishnaswamy H. Non-magnetic 60GHz SOI CMOS circulator based on loss/dispersion-engineered switched bandpass filters. 2019 IEEE International Solid-State Circuits Conference (ISSCC), 2019, 446

[32] Zhou J, Chuang T H, Dinc T, et al. Receiver with > 20MHz bandwidth self-interference cancellation suitable for FDD, co-existence and full-duplex applications. 2015 IEEE International Solid-State Circuits Conference (ISSCC), 2015, 1

[33] Reiskarimian N, Zhou J, Chuang T H, et al. Analysis and design of two-port N-path bandpass filters with embedded phase shifting. IEEE Trans Circuits Syst II, 2016, 63, 728

[34] van Liempd B, Hershberg B, Raczkowski K, et al. 2.2 A +70dBm IIP_3 single-ended electrical-balance duplexer in 0.18 μm SOI CMOS. 2015 IEEE International Solid-State Circuits Conference (ISSCC), 2015, 1

[35] Yang D, Yuksel H, Molnar A. A wideband highly integrated and widely tunable transceiver for in-band full-duplex communication. IEEE J Solid-State Circuits, 2015, 50, 1189

[36] Nagulu A, Chen T J, Zussman G, et al. Non-magnetic 0.18 μm SOI circulator with multi-watt power handling based on switched-capacitor clock boosting. 2020 IEEE International Solid-State Circuits Conference (ISSCC), 2020, 444

[37] He S, Akel N, Saavedra C E. Active quasi-circulator with high port-to-port isolation and small area. Electron Lett, 2012, 48, 848

[38] Huang D J, Kuo J L, Wang H E. A 24-GHz low power and high isolation active quasi-circulator. 2012 IEEE/MTT-S International Microwave Symposium Digest, 2012, 1

[39] Kim S, Kim Y. Multi octave wideband CMOS circulator using 0.11 μm process. 2013 European Microwave Integrated Circuit Conference, 2013, 204